R150A Mutant of F TraI Relaxase Domain: Reduced Affinity and Specificity for Single-Stranded DNA and Altered Fluorescence Anisotropy of a Bound Labeled Oligonucleotide†

Matthew J. Harley,‡ Dmitri Toptygin,‡ Thomas Troxler,# and Joel F. Schildbach*,‡

Department of Biology, The Johns Hopkins University, Baltimore, Maryland 21218, and Department of Chemistry, University of Pennsylvania, Philadelphia, Pennsylvania 19104

Received October 24, 2001

ABSTRACT: F factor TraI is a helicase and a single-stranded DNA nuclease ("relaxase") essential for conjugative DNA transfer. A TraI domain containing relaxase activity, TraI36, was generated previously. Substituting Ala for Arg150 (R150A) of TraI36 reduces in vitro relaxase activity. The mutant has reduced affinity, relative to wild type, for a 3′-TAMRA-labeled 22-base single-stranded oligonucleotide. While both R150A and wild-type TraI36 bind oligonucleotide, only wild type increases steady-state fluorescence anisotropy of the labeled 22-base oligonucleotide upon binding. In contrast, binding by either protein increases steady-state anisotropy of a 3′-TAMRA-labeled 17-base oligonucleotide. Time-resolved intensity data for both oligonucleotides, bound and unbound, require three lifetimes for adequate fits, at least one more than the fluorophore alone. The preexponential amplitude for the longest lifetime increases upon binding. Time-resolved anisotropy data for both oligonucleotides, bound and unbound, require two rotational correlation times for adequate fits. The longer correlation time increases upon protein binding. Correlation times for the protein-bound 17-base oligonucleotide are similar for both proteins, with the longer correlation time in the range of molecular tumbling of the protein−DNA complex. In contrast, protein binding causes less dramatic increases in correlation times for the 22-base oligonucleotide relative to the 17-base oligonucleotide. Binding studies indicate that R150 contributes to recognition of bases immediately 3′ to the DNA cleavage site, consistent with the apparent proximity of R150 and the 3′ oligonucleotide end. Models in which the R150A substitution alters single-stranded DNA flexibility at the oligonucleotide 3′ end or affects fluorophore−DNA or fluorophore−protein interactions are discussed.

Bacterial conjugation is the process by which a plasmid directs transfer of itself, in single-stranded form, from a donor to a recipient bacterium (for review, see refs *1* and *2*). For conjugative plasmid F Factor, *tra* (transfer) gene products direct this process. F TraI possesses a single-stranded DNA (ssDNA[1]) nuclease (or "relaxase") function that is required for transfer (*3*−*6*). Relaxases are named for their ability to relax supercoiled plasmid. TraI functions as part of a complex, the relaxosome (*7*, *8*), that also includes plasmid-encoded TraY and chromosome-encoded integration host factor (IHF). TraY and IHF specifically bind the F origin of transfer (*oriT*) and recruit TraI (*8*), possibly by inducing a local ssDNA conformation that TraI can recognize (*9*). In vitro, TraI binds and cleaves single-stranded, but not double-stranded, oligonucleotides sequence-specifically (*4*, *6*, *7*, *10*, *11*). During DNA cleavage, TraI forms a phosphotyrosyl linkage with one DNA strand in a transesterification reaction (*4*, *10*). The covalent link is formed between the protein and the DNA 3′ to *nic*, the site of DNA cleavage. The in vitro nicking reaction is easily reversible, suggesting that TraI may recircularize the transferred DNA strand (*2*, *12*). TraI, also known as DNA helicase I, is also a highly processive 5′-to-3′ helicase (*2*, *3*, *5*, *12*−*15*). This helicase activity, presumably used after TraI receives a signal indicating stable mating pair formation, unwinds the two plasmid strands prior to, or concurrent with, the 5′-to-3′ ssDNA transfer (*16*).

The structural and physical basis of ssDNA recognition and cleavage by relaxases is not well understood. We are examining function of the 192-kDa F TraI relaxase using an N-terminal 36-kDa fragment, TraI36, that retains in vitro relaxase activity (Street, et al., submitted). TraI36 binds an *oriT* ssDNA sequence with subnanomolar K_D and high sequence specificity (*11*).

F TraI is highly homologous to TraI from R100 (*17*) and shares limited homology with TrwC from R388 (*18*) and TraI from pKM101 (*19*). As part of an analysis of residues conserved among the four proteins, we generated the R150A mutant of F TraI36 and found that its in vitro relaxase activity

† This work was supported by National Science Foundation Grant MCB-9733655. The Regional Laser and Biotechnology Laboratories facility at the University of Pennsylvania is supported by National Institutes of Health Grant RR01348.

* Corresponding author: Phone: (410) 516−0176. Fax: (410) 516−5213. E-mail: joel@jhu.edu.

‡ Johns Hopkins University.

University of Pennsylvania.

[1] Abbreviations: kDa, kiloDalton; ssDNA, single-stranded DNA; TAMRA, carboxytetramethylrhodamine; bp, base pair; CPG, controlled pore glass; R150A, TraI relaxase domain mutant having Ala substituted for Arg at position 150; *oriT*, F factor origin of transfer; *nic*, site of TraI cleavage within *oriT* located between G140′ and T141′; IRF, instrument response function.

10.1021/bi011969i CCC: $22.00
Published on Web 04/27/2002

is reduced. Further experiments revealed that the substitution altered steady-state and time-resolved fluorescence characteristics of a bound fluorophore-labeled oligonucleotide relative to the those of an oligonucleotide bound to wild-type TraI36. Subsequent measurements of ssDNA binding indicated that the substitution causes a defined defect in binding specificity.

EXPERIMENTAL PROCEDURES

Mutagenesis. The R150A TraI36 mutant was engineered by site-directed PCR mutagenesis of plasmid pET24a-*traI36* (Street, et al., submitted) as described (*20*). Primers used were 441-SPE (5′-CGCACTAGTGTCGTGGTTAAACAGTGC-CAT-3′) and R150A (5′-CGGACTAGTGCCGATCAGG-AACCACAGTTAC-3′). Primers encoded a silent, unique *Spe*I site (underlined) for generating circular plasmid from PCR product by ligation, and for screening putative mutants. Mutated *traI36* genes were sequenced, and the plasmids were transformed into BL21(DE3) cells for protein expression.

Protein Purification. Wild-type TraI36 was expressed and purified as described (Street, et al., submitted). R150A TraI36 was purified similarly, except that protein-containing pre-elution heparin column fractions and the elution peak were combined and loaded onto the blue column.

Oligonucleotide Synthesis and Purification. Oligonucleotides were purchased from Integrated DNA Technologies, Inc. Wild-type TraI binding site oligonucleotides are 5′-TTTGCGTGGGGTGTGGTGCTTT-3′ (22-base, or FTAM (*11*)), 5′-TTTGCGTGGGGTGTGGT-3′ (17-base), and 5′-TTTGCGTGGGGTGT-3′ (14-base). Variant oligonucleotides are G147′A (5′-TTTGCGTAGGGTGTGGTGCTTT-3′), G140′C (5′-TTTGCGTGGGGTGTCGTGCTTT-3′), G140′A (5′-TTTGCGTGGGGTGTAGTGCTTT-3′), and G139′T (5′-TTTGCGTGGGGTGTGTTGCTTT-3′), with substitutions underlined. The nonspecific oligonucleotide is 5′-ATAAAGAGAGTAAGAGAAACTA-3′. TAMRA labels were incorporated at the 3′ end by use of TAMRA-CPG columns, or at the 5′ end using an *N*-hydroxysuccinimide ester linkage to a 5′-amino-modified oligonucleotide. Labeled oligonucleotides were purified by polyacrylamide gel electrophoresis as described (*21*).

Protein Characterization. Relative relaxase function was assessed by a radioactive nicking assay (*12*) as described (*11*), except that in some experiments time points of cleavage by 200 nM protein were collected over a 60-min period. Circular dichroism (CD) wavelength spectra and thermal denaturation data were collected with a Jasco J-710 spectropolarimeter as described (Street, et al., submitted).

Fluorescence-Based Characterization of DNA Binding. Affinity measurement by protein titration into solutions of fluorophore-labeled oligonucleotide was as described (*11*). Data were fit using SPECTRABIND (*22*, *23*), a global fitting algorithm for linear-response equilibrium binding data. For each titration point, intensity (I) and the sum of intensity and anisotropy (r), both of which are linear in the concentrations of individual fluorescent species, were fit simultaneously. The program requires a variance (squared standard deviation) for each experimental quantity. Inverse variances are used as weights by the nonlinear least-squares algorithm, and variances are also involved in calculating χ^2 values. Estimated standard deviations used in most fits were $\sigma I = 0.01I$, $\sigma r = 0.001$, $\sigma(rI) = [(r\sigma I)^2 + (\sigma rI)^2]^{1/2}$, and $\sigma c = 0.01c$, where c is titrant concentration. For R150A titrations into the 3′-labeled 22-base oligonucleotide, $\sigma r = 0.1$ was used to de-emphasize the anisotropy data, which is equivalent to fitting the intensity data alone.

Binding specificity was assessed by competition with unlabeled oligonucleotides as described (*11*) with 4 nM 3′-TAMRA-labeled 22-base oligonucleotide and either 4 nM wild-type TraI36 or 70 nM R150A, concentrations that yield approximately half-maximal DNA binding. IC_{50} values were obtained by fitting data using Kaleidagraph 3.0 (Synergy Software) with the formula $IC_{50} = [(U_i + U_s \log(C)) - L_i]/[1 + (IC_{50}/C)]$ where IC_{50} is the competitor concentration inhibiting 50% of binding, C is competitor oligonucleotide concentration, U_i is upper intercept, U_s is slope of the upper baseline, and L_i is lower intercept. Some curves have slight baseline slopes that appear linear with the log of the concentration (*11*). The slope term was used only when the upper baseline had an apparent slope and inclusion of the term was judged to improve the quality of the fit.

Time-resolved anisotropy and intensity were measured at the Regional Laser and Biotechnology Laboratories facility at University of Pennsylvania. Frequency-doubled output from a YAG:Nd pumped dye laser (Coherent Antares) was used for excitation. The dye solution contained Rhodamine 6G in ethylene glycol. Measurements were taken at ambient temperature. The emission polarizer was oriented at the magic angle for intensity decay sets, and 0° or 90° relative to the polarization of the laser pulse for anisotropy decay sets. TAMRA was excited at 565 nm and emission observed at 595 nm. Decay curves were obtained by time-correlated single-photon counting. One channel of the multichannel analyzer was equivalent to 22.7 ps, and data were collected over approximately 10 ns following each excitation pulse. Samples contained 100 nM oligonucleotide and 300 nM wild-type TraI36, 500 nM R150A TraI36, or no protein. Intensity decay data were analyzed using the single-curve fitting program TCPHOTON (*24*), allowing time constants, preexponential amplitudes, constant photomultiplier background, and time shift between decay curves and instrument response function (IRF) to vary as free fitting parameters. Although the IRF was measured immediately before the fluorescence data collection, use of this value led to suboptimal fits, especially in the leading edge of the decay curves. Suspecting IRF drift between measurements of scattering solution and fluorescent samples, we used a previously collected, more characteristic IRF, which markedly improved the quality of the fits.

Time-resolved anisotropy data were fit using the global analysis program POLARTCP (*24*). Preexponential factors (β_m) and rates ($1/\phi_m$) corresponding to anisotropy, preexponential factors (α_n), and rates ($1/\tau_n$) corresponding to the total intensity, and the ratio of instrument sensitivity to vertical and horizontal polarization (g-factor) were treated as free fitting parameters. Steady-state anisotropy (r_{ss}) was used as a constraint. r_{ss} was measured using a SLM Aminco 48000MHF spectrofluorometer configured in L format. Excitation and emission monochromator slits were set to 8 nm spectral width. Three sets of 20 instrument averages were collected for the measured intensities I_{vv}, I_{vh}, I_{hh}, and I_{hv}, where the first subscript indicates the orientation, vertical (v) or horizontal (h), of the excitation polarizer, and the

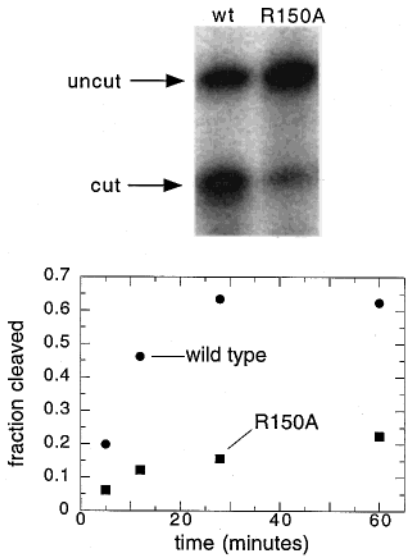

FIGURE 1: R150A substitution reduces TraI36 relaxase activity relative to wild type. A representative time course using 200 nM protein and 100 pM 5′ ^{32}P-labeled single-stranded oligonucleotide is shown. Upper: bands corresponding to the 28-min time point are shown. The upper band is the uncut 22-base oligonucleotide and the lower band is the 5′ 14-base oligonucleotide cleavage product. Lower: The bands are quantitated and graphed as fraction cleaved versus time. Wild-type TraI (circles) generates more product at this protein concentration than does R150A (squares).

second indicates orientation of the emission polarizer. The calculation used the following equation: $r_{ss} = (I_{vv}I_{hh} - I_{vh}I_{hv})/(I_{vv}I_{hh} + 2I_{vh}I_{hv})$. The 99% confidence intervals of time-resolved anisotropy parameter values were estimated by plotting reduced χ^2 values versus parameter values. Fits were repeated with a fixed parameter value (β or ϕ), while other parameters were allowed to float. According to F-distribution, with the probability of $(1 - p)$ the value of the one parameter ($\upsilon_1 = 1$) that is fixed during the χ^2 minimization must be within the interval where $\chi^2 = ([1 + (\upsilon_1/\upsilon_2)F(p,\upsilon_1,\upsilon_2)]\chi^2_{min})$. Here υ_2 represents the number of analyzer channels with nonzero weights less the number of free fitting parameters, in our case, $\upsilon_2 = 1000 - 14$. With this value of υ_2 and $p = 0.01$ (99% confidence), the condition of the fixed parameter value being within the confidence interval reduces to $\chi^2 = (1.0067\chi^2_{min})$. This condition was used to determine the confidence intervals.

RESULTS

Reduced Cleavage Activity of R150A TraI36 Mutant. The TraI36 mutant R150A was generated as part of a project examining residues conserved among four related relaxases. In an initial screen, in vitro DNA cleavage by wild-type and R150A TraI36 were compared (Figure 1). In this assay, cleavage is observed by conversion of a 5′ radiolabeled 22-base ssDNA oligonucleotide substrate into a 14-base labeled fragment. R150A activity is reduced relative to wild type, with 200 nM R150A yielding approximately one-third of the product generated by 200 nM wild-type TraI36. In an equilibrium cleavage assay using a range of protein concentrations, increasing the concentration of R150A 100-fold relative to that of wild-type TraI36 yields similar levels of ssDNA cleavage (data not shown). Wild-type and R150A TraI36 have similar circular dichroism (CD) wavelength spectra, and have similar thermal denaturation curves when

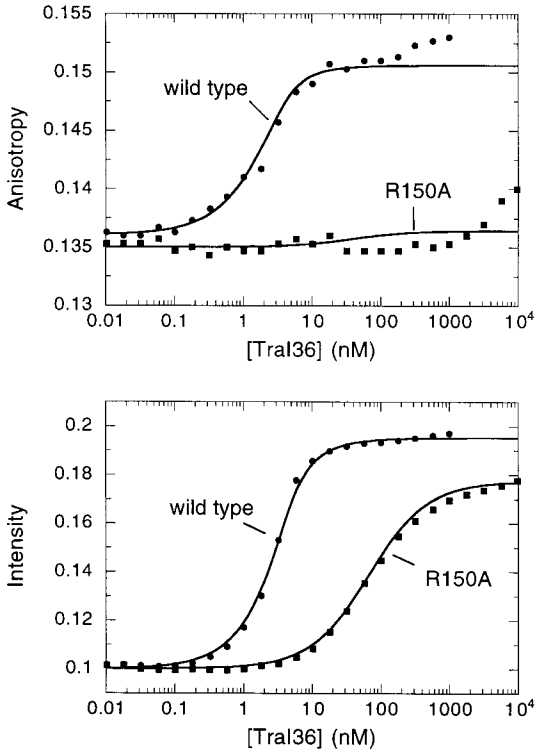

FIGURE 2: Comparison of R150A (squares) and wild-type TraI36 (circles) binding to 3′-TAMRA-labeled 22-base oligonucleotide. Curves show changes in anisotropy (upper) and total emission intensity (lower) upon binding. Oligonucleotide concentration is initially 4 nM. Intensity data are adjusted for fluorophore dilution and normalized for initial intensity (arbitrary units) relative to each other. Fits were generated with SPECTRABIND (*22*, *23*) using data points through 180 nM wild-type TraI36 and 10 μM R150A TraI36.

denaturation is followed by loss of CD ellipticity (Supporting Information, Figure 1). These results suggest that the reduced relative cleavage activity of R150A does not result from improper folding or reduced protein stability.

Reduced ssDNA Affinity of R150A and Altered Steady-State Fluorescence Anisotropy of Bound Oligonucleotide. To test whether the reduced apparent activity of R150A was due to reduced binding of ssDNA, the affinities of R150A and wild-type TraI36 for the TraI *oriT* binding site were measured by following changes in steady-state fluorescence intensity and anisotropy of different fluorophore-labeled oligonucleotides upon titration of the protein. The relaxase cleavage activity requires Mg^{2+}, and because these experiments were performed in absence of Mg^{2+}, the data shown represent reversible binding reactions. When using a 4 nM solution of 3′-TAMRA-labeled 22-base oligonucleotide, binding of wild-type TraI36 increases steady-state anisotropy and emission intensity of the labeled oligonucleotide (Figure 2). The titration contains a transition with a midpoint at approximately 3 nM, which corresponds to specific binding (*11*). A second, more variable increase begins at approximately 300 nM, and appears to be due to nonspecific interactions (*11*). Fitting intensity and anisotropy data from five assays through 180 nM protein with SPECTRABIND (*22*, *23*) yields an average K_D of 0.43 nM for wild-type TraI36 binding the 22-base oligonucleotide (Table 1).

Results from the R150A titration indicate that the mutant protein has a different effect on steady-state anisotropy of the bound oligonucleotide relative to wild type, and also has

Table 1: Dissociation Constants of Wild-Type and R150A TraI36 for 22-Base and 17-Base 3′-TAMRA-Labeled Oligonucleotides[a]

3′-TAMRA-labeled oligonucleotide	K_D (nM)	
	wild-type TraI36	R150A TraI36
22-base	0.43 ± 0.30 (5)	57 ± 17 (5)
17-base	0.74 ± 0.38 (4)	33 ± 6.3 (6)

[a] K_D values were obtained by fitting steady-state intensity and anisotropy data from protein titrations into 4 nM oligonucleotide using the program SPECTRABIND (*22*, *23*) and are shown as averages with standard deviations. Number of experiments averaged for each sample is shown in parentheses.

reduced affinity for ssDNA. As shown in Figure 2, titrating R150A into a 4 nM solution of the 3′-TAMRA-labeled 22-base oligonucleotide increases total emission intensity of the bound, labeled oligonucleotide, but does not substantially affect the fluorescence anisotropy of the oligonucleotide. The increase in intensity is apparently due to specific recognition, since the intensity decreases upon addition of an unlabeled oligonucleotide with the same sequence, but not by addition of an oligonucleotide with a different sequence (Supporting Information, Figure 2). Using SPECTRABIND with parameters that heavily weight the intensity data relative to anisotropy data (see Experimental Procedures) to fit results from five assays through 10 μM protein yields an average K_D of R150A TraI36 for the 22-base oligonucleotide of 57 nM (Table 1). The reduced affinity of R150A for ssDNA correlates well with the apparent reduction in nicking by R150A seen in the in vitro nicking assay.

To test whether the failure of the R150A mutant to increase fluorescence anisotropy of the 3′-TAMRA-labeled 22-base oligonucleotide was specific to the location of the fluorophore on the DNA, we first examined the effect of R150A binding to a 3′-TAMRA-labeled 17-base oligonucleotide. This oligonucleotide lacks the five bases at the 3′ end of the 22-base oligonucleotide, but is otherwise identical. Wild-type TraI36 binds the 17- and 22-base oligonucleotides with similar affinities (Table 1; *11*). In contrast to the results for the 22-base oligonucleotide, both R150A and wild-type TraI36 increase steady-state fluorescence emission intensity and anisotropy of the 17-base oligonucleotide (Figure 3). R150A exhibits similar reductions in affinity for the 17- and 22-base oligonucleotides, relative to wild-type TraI36 (Table 1).

As a second test of the effect of the fluorophore location, these experiments were repeated with 17- and 22-base oligonucleotides with a 5′ TAMRA label. As before, R150A demonstrated reduced affinity for both oligonucleotides relative to wild-type TraI36 (not shown). Both proteins, however, caused similar increases in fluorescence anisotropy and intensity of the TAMRA probe upon binding. In summary, wild-type and R150A TraI36 differ in their effects on anistropy of the 3′-TAMRA-labeled 22-base oligonucleotide, but both increase emission intensity of this labeled oligonucleotide similarly. The two proteins increase both anisotropy and intensity of all the other labeled oligonucleotides examined to similar extents.

Time-Resolved Fluorescence Emission Intensity and Anisotropy. To further characterize the different effects of wild-type and R150A TraI36 on anisotropy of the 22-base oligonucleotide, time-resolved intensity and anisotropy experiments were performed using the 3′-TAMRA-labeled 17- and 22-base oligonucleotides, unbound and with bound

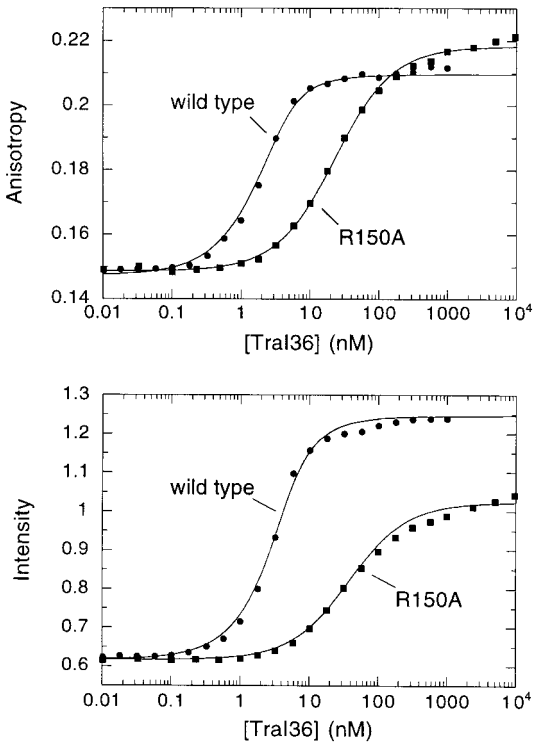

FIGURE 3: Curves for 3′-TAMRA-labeled 17-base oligonucleotide showing changes in anisotropy (upper) and total intensity (lower) upon binding of wild-type (circles) and R150A (squares). Oligonucleotide concentration is initially 4 nM. Intensity data are adjusted for fluorophore dilution and normalized for initial intensity (arbitrary units) relative to each other. Fits were generated with SPECTRABIND (*22*, *23*) using data points through 180 nM wild-type TraI36 and 10 μM R150A.

Table 2: Parameter Values for Time-Resolved Intensity Measurements[a]

3′-TAMRA-Labeled 22-Base Oligonucleotide								
protein	τ_1 (ns)[b]	%α_1[c]	τ_2 (ns)	%α_2	τ_3 (ns)	%α_3	χ^2 [d]	$I(t)$[e]
none	0.23	42.0	0.92	28.5	3.2	29.5	1.57	1.30
wild type	0.36	20.0	1.5	26.0	3.4	54.1	1.35	2.30
R150A	0.35	29.5	1.4	26.0	3.3	44.5	1.33	1.94
3′-TAMRA-Labeled 17-Base Oligonucleotide								
protein	τ_1 (ns)	%α_1	τ_2 (ns)	%α_2	τ_3 (ns)	%α_3	χ^2	$I(t)$
none	0.33	35.4	1.1	36.9	2.9	27.6	1.53	1.32
wild type	0.47	21.1	1.8	31.7	3.5	47.2	1.38	2.32
R150A	0.34	25.3	1.3	33.6	3.4	41.1	1.31	1.92
TAMRA								
protein	τ_1 (ns)		%α_1	τ_2 (ns)		%α_2	χ^2	
none	0.14		8.8	2.2		91	1.47	

[a] Fits were made using the program POLARTCP (*24*). [b] τ: intensity lifetimes in ns. [c] %α: percentage of the preexponential amplitude. [d] χ^2: reduced chi square values for the fits. [e] α-averaged intensity lifetime values, where $I(t) = \sum_i^n \alpha_i \exp(-t/\tau_i)$.

R150A or wild-type TraI36. The intensity decay curves were fit by sums of exponential functions using the program TCPHOTON (*24*), and parameter values that resulted in the best fits are shown in Table 2. The intensity decay curve and the corresponding fit for wild-type TraI36 bound to the 22-base oligonucleotide are shown in Figure 4, and each of the other intensity decay curves are provided in the Supporting Information (Supporting Information, Figures 3−7). The fits describe the data well, although the

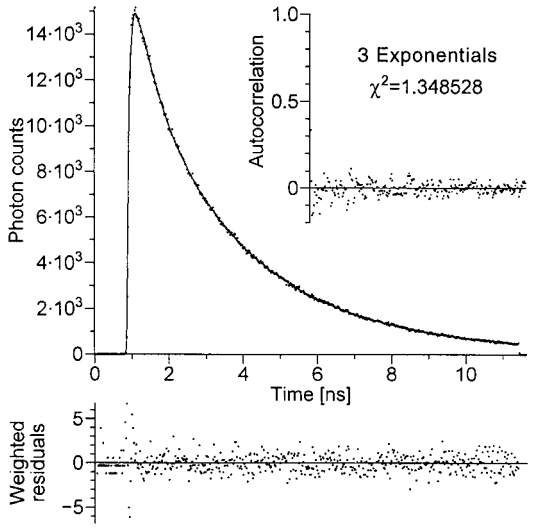

FIGURE 4: Time-resolved emission intensity of the TAMRA-labeled 22-base oligonucleotide (100 nM) bound to wild-type TraI36 (300 nM). The experimental data points and the fit decay curves (upper panel) generated using TCPHOTON (*24*) are shown with the weighted residuals (lower panel) and the normalized autocorrelation of residuals (inset). The other intensity decay curves are located in the Supporting Information.

greatest residuals for the fit are consistently for data points located near the leading edge of the peak. These larger residuals may be due to a small time shift during data collection, or to a small contribution by light scattering.

The best fits to all the intensity decay curves from the TAMRA-labeled oligonucleotides, bound and unbound, require three lifetimes (τ). These lifetimes are on the order of 0.33, 1.4, and 3.3 ns for each sample, and each lifetime had a substantial ($\geq$20%) preexponential amplitude (α). Because one lifetime would be expected from a homogeneous solution where the fluorophore is free from quenching interactions, the multiple lifetimes suggest that the population of TAMRA molecules is exposed to a heterogeneous environment, possibly by adopting different orientations with respect to the DNA. Previous time-resolved fluorescence studies of 5′-TAMRA-labeled oligonucleotides showed multiple lifetimes that were similar to the fast and slow (τ_1 and τ_3) lifetimes that we observe (*25*, *26*). Previous time-resolved intensity measurements of rhodamine dyes yielded one or two lifetimes under different conditions (*27*, *28*). Analysis of our time-resolved intensity measurements of a mixture of 5- and 6-carboxytetramethylrhodamine (5- and 6-TAMRA) isomers gave two intensity decay lifetimes, 0.14 and 2.2 ns, having preexponential amplitudes of 9 and 91%, respectively (Table 2). Because the short lifetime is half the length of any other observed, and the preexponential amplitude is half that of any other observed, we suspect that this lifetime may represent solvent relaxation (*29*), sample heterogeneity, or some experimental artifact. Regardless, the TAMRA-labeled oligonucleotides demonstrate at least one more lifetime than the dye alone, consistent with the probe existing in multiple conformations when linked to the oligonucleotide.

The time-resolved intensity data explain the increased steady-state emission intensity of the 3′-TAMRA-labeled oligonucleotides upon protein binding. First, intensity lifetimes are similar or longer for bound oligonucleotides relative to unbound oligonucleotides. For example, τ_3 is 2.9 ns for

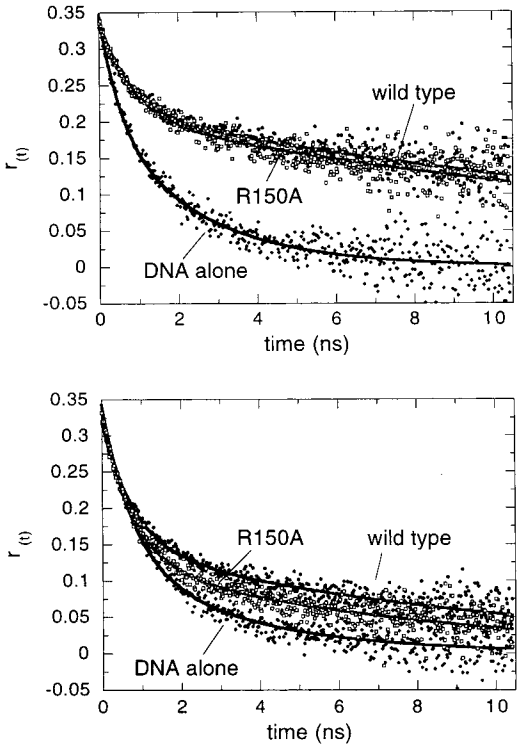

FIGURE 5: Time-resolved anisotropy curves differ for R150A and wild-type TraI36 bound to the 22-base, but not the 17-base, oligonucleotide. The fits (solid lines) were made using POLARTCP (*24*) and are overlayed on the points obtained from channel-by-channel calculations of the vertical and horizontal polarization data. DNA alone (filled diamonds), 300 nM wild-type TraI36 (filled circles), and 500 nM R150A TraI36 (open squares) samples are shown for the 17-base oligonucleotide (upper) and the 22-base oligonucleotide (lower).

the unbound 17-base oligonucleotide, but 3.5 and 3.4 ns when bound by wild-type and R150A TraI36, respectively (Table 2). Second, the amplitude of the longest lifetime (α_3) is increased for the protein-bound oligonucleotides relative to the unbound oligonucleotides, while decreased for the shortest lifetime (α_1). The amplitude for τ_3 of the unbound 17-base oligonucleotide is 28% (percentage of total amplitude), while it is increased to 47 and 41% for that bound by wild-type and R150A TraI36, respectively. The combination of these factors increases steady-state intensity of the bound versus unbound oligonucleotides.

Time-resolved anisotropy data and the corresponding fits are shown in Figure 5. Vertical and horizontal components of the decay curves were simultaneously fit using the global fitting program POLARTCP (*24*). Each oligonucleotide curve fit well with two rotational correlation times (ϕ), while the data for the dye alone fit well with a single rotational correlation time. Correlation times and preexponential amplitudes (β) of the time-resolved anisotropy curves are listed in Table 3.

Comparing curves (Figure 5) and values derived from fits to the curves (Table 3) for the two unbound oligonucleotides reveals that they exhibit similar behavior, despite differences in length and mass. The confidence intervals of most parameters for the two unbound oligonucleotides overlap, although the longer correlation time for the 17-base oligonucleotide (ϕ_2 = 2.4 ns; 99% confidence interval = 2.2−2.8) is slightly but significantly shorter than the ϕ_2 value for the 22-base oligonucleotide (3.3 ns; 3.0−4.0).

Table 3: Parameter Values for Time-Resolved Anisotropy Measurements[a]

3′-TAMRA-Labeled 22-Base Oligonucleotide							
protein	$r(t=0)$[b]	r (ss)[c]	ϕ_1 (ns)[d]	β_1[e]	ϕ_2 (ns)	β_2	χ^2 [f]
none	0.343	0.139	0.76	0.21	3.3	0.13	1.77
wild type	0.320	0.153	0.78	0.17	10	0.15	2.80
R150A	0.333	0.142	0.74	0.20	7.7	0.13	2.15
3′-TAMRA-Labeled 17-Base Oligonucleotide							
protein	$r(t=0)$	r (ss)	ϕ_1 (ns)	β_1	ϕ_2 (ns)	β_2	χ^2
none	0.347	0.147	0.52	0.14	2.4	0.20	2.01
wild type	0.341	0.213	0.73	0.13	19	0.22	2.70
R150A	0.338	0.213	0.83	0.13	18	0.21	2.66
TAMRA							
protein	$r(t=0)$	r (ss)	ϕ_1 (ns)	β_1	χ^2		
none	0.346	0.0307	0.21	0.35	2.30		

[a] Fits were made using the program POLARTCP (*24*). [b] $r(t=0)$: anisotropy at $t = 0$. [c] r (ss): steady-state anisotropy. [d] ϕ: correlation time in ns. [e] β: preexponential amplitude. [f] χ^2: reduced chi square values for the fits.

Table 4: Affinities of R150A and Wild-Type TraI36 for Variant Oligonucleotides as Determined by Competition Assay[a]

	wild-type TraI36			R150A		
oligonucleotide	IC_{50} (nM)	n	relative IC_{50}	IC_{50} (nM)	n	relative IC_{50}
22-base	9.1 ± 0.6	3	1.0	170 ± 20	4	1.0
14-base	120 ± 29	3	13	54 ± 25	4	0.32
G140′C	240 ± 91	3	26	250 ± 31	3	1.5
G140′A	68 ± 16	2	7.4	210 ± 35	2	1.2
G139′T	12 ± 0.1	2	1.4	130 ± 60	2	0.8
G147′A	640 ± 280	3	70	3200 ± 580	3	19

[a] Binding is expressed as IC_{50}, the concentration of unlabeled oligonucleotide required to compete away 50% of binding of the labeled oligonucleotide. Relative IC_{50} values, which compare an IC_{50} value to that of the protein for the 22-base oligonucleotide, are also given. Values from multiple (n) experiments were averaged for each sample with the standard deviation shown.

Comparing curves (Figure 5) and values resulting from the best fits to these data (Table 3) for the 17-base oligonucleotide bound to wild-type or R150A TraI36 suggests that the increased steady-state anisotropy of the bound oligonucleotide is due to a significant increase in ϕ_2. The correlation time, with 99% confidence intervals given in parentheses, rises from 2.5 (2.2−2.8) ns for unbound oligonucleotide to 19 (16−25) and 18 (14−25) ns for oligonucleotide bound to wild-type and R150A TraI36, respectively. The small increase in ϕ_1 for bound relative to unbound oligonucleotides and the differences in the preexponential amplitudes are not significant.

In contrast, the 22-base oligonucleotide shows less striking, yet still significant, increases in ϕ_2 upon binding to protein, explaining the smaller steady-state anisotropy changes for bound 22-base relative to bound 17-base oligonucleotides (Figures 2 and 3; Table 3). ϕ_2 is 3.3 (3.0−4.0) ns for the unbound 22-base oligonucleotide, and 10 (8.3−12) and 7.7 (6.3−9.4) ns for the oligonucleotide bound by wild-type and R150A TraI36, respectively. The amplitudes for these ϕ_2 values (β_2) are similar. The ϕ_1 values are also similar for unbound and protein-bound oligonucleotides. β_1 for the wild-type-bound oligonucleotide (0.17; 99% confidence interval = 0.16−0.18) is smaller than that for the unbound (0.21; 0.15−0.24) and R150A-bound (0.20; 0.19−0.21) oligonucleotide, but the difference is significant only between values for the bound oligonucleotides. Although the increase in ϕ_2 for the 22-base oligonucleotide upon binding of R150A is significant, its effect on steady-state anisotropy is apparently too small to be detected above the noise in our binding measurements by protein titration (Figure 2). Binding by wild-type TraI36 increases steady-state anisotropy detectably, and a reduced β_1 relative to that for R150A-bound oligonucleotide may contribute to this difference. There is a larger β_2 and greater relative increase in ϕ_2 than occurs with R150A, but the overlapping confidence intervals makes the significance of these changes questionable.

Contribution of R150 to Recognition of DNA 3′ to Nic. The reduced affinity of R150A TraI36 for ssDNA indicates that R150 contributes to DNA recognition. There are two observations suggesting that R150 contributes to recognition of bases 3′ to *nic*, the TraI cleavage site at *oriT*. First, the R150A substitution alters the anisotropic characteristics of a bound 3′-labeled 22-base oligonucleotide (Figure 2). In contrast, binding by R150A and wild-type TraI36 similarly affect the anisotropy of a 5′-labeled 22-base oligonucleotide (not shown). The differences in anisotropy are likely to be due to changes in relatively short-range interactions, suggesting R150A has altered recognition of one or more of the 8 oligonucleotide bases 3′ to *nic*, rather than of one of the 14 bases 5′ to *nic*. Second, the protein concentration dependence of oligonucleotide cleavage by R150A suggests that protein−DNA interactions 3′ to *nic* have been altered. In equilibrium oligonucleotide cleavage assays using wild-type TraI36 and an unsubstituted oligonucleotide, TraI36 binds and partially cleaves the oligonucleotide at low (nM) protein concentrations, but does not completely cleave the oligonucleotide until high (μM) TraI36 concentrations are reached (*11*). When variant oligonucleotides containing affinity-reducing base substitutions are used, higher TraI36 concentrations are required to see any cleavage, consistent with the reduced affinity of the protein for substrate. If the affinity-reducing substitutions are located 3′ to *nic*, the oligonucleotide is only partially cleaved over a wide TraI36 concentration range, just like is observed with the unsubstituted oligonucleotide. In contrast, oligonucleotides having affinity-reducing substitutions 5′ to *nic* are completely cleaved by TraI36 over a narrow protein concentration range (*11*). We attributed these results to the increased dissociation rate constant for the 5′ cleavage product of the variant oligonucleotide from the protein, which favors dissociation over ligation (the reverse reaction), relative to the unsubstituted DNA sequence. As expected given the reduced R150A affinity, a higher R150A concentration is required to observe oligonucleotide cleavage than for wild type (Figure 1 and data not shown). The R150A mutant, however, shows incomplete cleavage over a considerable protein concentration like wild-type TraI36 (data not shown), consistent with the lost protein−DNA interactions being located 3′ to *nic*.

To test R150A for loss of interactions with DNA 3′ to *nic*, we analyzed the binding specificities of wild-type and R150A TraI36 by competition assay. Binding of wild-type and R150A TraI36 to variant oligonucleotides expressed as IC_{50} values (concentration of competitor that reduced binding of TAMRA-labeled oligonucleotide by 50%), are given in Table 4. To obtain adequate fluorescence signal, we used

protein concentrations near or above the measured K_D of the interaction, and, for wild-type TraI36, oligonucleotide concentrations above the K_D of the interaction, raising the IC_{50} values above the actual K_D values (*30*).

The IC_{50} of the 22-base oligonucleotide for wild-type TraI36 is 9 nM (Table 4). A 14-base oligonucleotide lacking bases 3′ to *nic* is bound with reduced affinity as shown by the 13-fold increase in IC_{50}. In contrast, R150A binds the 14-base oligonucleotide (IC_{50} = 54 nM) slightly better than the 22-base oligonucleotide (IC_{50} = 170 nM). Wild-type TraI36 binds G140′C and G140′A variant oligonucleotides, which have their base substitutions located 3′ to *nic*, with measurably reduced affinity (26- and 7-fold higher IC_{50} values, respectively) relative to the unaltered DNA sequence. The R150A mutant, however, binds these variant oligonucleotides with affinities similar to that of the unsubstituted 22-base oligonucleotide. Both wild-type and R150A TraI36 bind the G139′T variant with affinities similar to those for the unsubstituted oligonucleotide. The binding characteristics of the R150A mutant are not due simply to an overall reduction in specificity. Both wild-type and R150A TraI36 bind the G147′A variant oligonucleotide, which has a substitution 5′ to *nic*, with significantly reduced affinity relative to the unaltered 22-base oligonucleotide. Therefore, the binding of both wild-type and R150A TraI36 is sensitive to base substitutions 5′ to *nic* (G147′C), but only wild type is sensitive to substitutions 3′ to *nic* (14-base, G140′C, and G140′A).

DISCUSSION

Contribution of R150 to Binding Affinity and Specificity of TraI36. R150 of the F factor TraI relaxase domain contributes to the affinity and specificity of ssDNA recognition. Substitution of Ala (Figures 2 and 3; Table 1) or Cys (not shown) for the conserved R150 amino acid reduces the affinity of the mutant 100-fold, relative to that of wild type, for an oligonucleotide containing the TraI specific binding site. Results from competition assays (Table 4) indicate that R150 contributes to recognition of at least one base located immediately 3′ to *nic*.

Arg can interact with ssDNA in myriad ways as shown by the structures of sequence-specific ssDNA binding proteins *Oxytricha nova* telomere end binding protein (*31*−*33*) and human heterogeneous nuclear ribonucleoprotein A1 (*34*). These include forming salt bridges with phosphodiester groups in the DNA backbone, hydrogen bonds with DNA, and cation-π-type interactions with the bases. The versatility of the Arg side chain, coupled with the possibility that Arg can simultaneously participate in multiple interactions with DNA, suggests how a single amino acid substitution could alter both affinity and specificity of TraI36 ssDNA recognition.

While the R150A mutant has reduced binding specificity, the contribution of R150 to TraI36 specificity is relatively modest. First, although the R150 residue is conserved among the TraI proteins of F, R100 and pKM101, and the TrwC protein of R388 (*2*, *17*−*19*), the 2 bases 3′ to *nic* in these plasmids are not (*35*). In F and R100, the sequence is 5′-GG-3′, while in R388 and pKM101 the sequence is 5′-AT-3′. F TraI36 can bind well to sequences with either of these two base changes, with affinity reduced by less than 10-fold (Table 4). Second, R150 contributes to recognition of bases 3′ to *nic*, but base substitutions at some positions 5′ to *nic* have considerably larger effects on wild-type TraI36 binding than equivalent substitutions 3′ to *nic* (*11*). So while the R150A mutant has lost recognition of sequences 3′ to *nic*, the lost interactions contribute only modestly to the overall specificity of the TraI36−ssDNA interaction.

Correlation of Steady-State and Time-Resolved Fluorescence Emission Intensity Data. The fluorescence emission intensity of both the 17-base and the 22-base 3′-TAMRA-labeled oligonucleotides increases upon binding by wild-type or R150A TraI36 (Figures 2 and 3). Time-resolved intensity data for the unbound oligonucleotides require three lifetimes for an adequate fit, at least one more than for the dye alone (Table 2). The multiple lifetimes suggest that the fluorophore can adopt different orientations relative to the oligonucleotide, and the fluorophore has somewhat different environments in these orientations. The time-resolved intensity data suggest that the increase in steady-state intensity upon binding by the proteins is attributable to a greater amplitude for the longest lifetime, a smaller amplitude for the shortest lifetime and, in some cases, an increase in the lifetimes. These differences could be due to factors including direct fluorophore−protein interactions, altered fluorophore−DNA interactions in the presence of the bound protein, or a changed fluorophore environment caused by an alteration in local ssDNA conformation upon binding. Possible fluorophore−DNA interactions include electrostatic interactions between the dimethylamine groups or the carboxyphenolic group of the dye and the charged or polar groups of the DNA, and face-to-face stacking interactions between the dye and the 3′ DNA base (*26*).

Role of R150 in Anisotropy of a Bound Fluorophore-Labeled Oligonucleotide. While the binding of R150A TraI36 increases the fluorescence intensity of a 3′-TAMRA-labeled, 22-base oligonucleotide, bound R150A has little corresponding effect on the steady-state anisotropy of the fluorophore (Figure 2). In contrast, wild-type TraI36 increases both total fluorescence emission intensity and steady-state anisotropy of the 3′-labeled 22-base oligonucleotide. R150A and wild-type TraI36 both increase steady-state fluorescence intensity and anisotropy of a 3′-TAMRA-labeled 17-base oligonucleotide (Figure 3), and the steady-state anisotropy values for the bound 17-base oligonucleotide are larger than those observed for the 22-base oligonucleotide. Time-resolved anisotropy data indicate that wild-type and R150A TraI36 cause significant increases in the longer correlation time (ϕ_2) upon binding to either oligonucleotide. The significantly greater ϕ_2 for the bound 17-base oligonucleotide than the bound 22-base oligonucleotide largely explains the differences in their steady-state anisotropy values.

The cause of the different steady-state anisotropy levels for the 3′-labeled 22-base oligonucleotide when bound by R150A and wild-type TraI36 is more difficult to identify. There is a small but significant difference in β_1 for the R150A- and wild-type-bound oligonucleotides, which may account for at least some of the difference. The ϕ_2 and β_2 values are smaller for the R150A-bound relative to the wild-type-bound 22-base oligonucleotide, suggesting that they might contribute to the difference, but the confidence intervals for these values partially overlap, making their roles uncertain.

The anisotropy data indicate that the fluorophore of the protein-bound 17-base oligonucleotide is more constrained than that of the bound 22-base oligonucleotide. The ϕ_2 for the 17-base oligonucleotide, bound by either wild-type or R150A TraI36, is approximately 18 ns. An unhydrated hard sphere of the molecular weight of the complex of TraI36 and the 17-base oligonucleotide (~41.5 kDa) would have a rotational correlation time on the order of 12 ns (*36*). Hydration and deviations from a spherical shape should increase the rotational correlation time, with the actual correlation time as much as twice the calculated value. The ϕ_2 for the bound 17-base oligonucleotide is therefore on the order of the rotational correlation time for the complex, suggesting that the motion of a subset of the fluorophore population is relatively constrained.

In contrast, the ϕ_2 values for the 22-base oligonucleotide are 10 and 7.7 ns when bound by wild type and R150A, respectively. If the anisotropy of the bound state reflected only the global tumbling of the complex, we would expect similar ϕ_2 values for both 17- and 22-base oligonucleotides. Anisotropy, however, reflects both the local motion of the fluorophore and the global motion of the complex. The smaller ϕ_2 values for the 22-base oligonucleotide are consistent with the fluorophore of the bound 22-base oligonucleotide being less constrained and having greater local motion.

There are at least three models that might explain the anisotropy data, all relating to the local environment of the fluorophore. These models are not mutually exclusive, nor do we have sufficient data to distinguish between them. The first model invokes increased segmental flexibility at the 3′ end of the 22-base oligonucleotide. The similar affinities of TraI36 for the 22- and 17-base oligonucleotides suggest that the 5 bases at the 3′ end of the 22-base oligonucleotide do not interact significantly with the protein. The motion of these bases may therefore be relatively unrestricted. If so, this additional segmental mobility of the 3′ DNA bases may contribute to the reduced ϕ_2 for the 3′-labeled 22-base oligonucleotide.

In a second model, protein−flurophore interactions could affect fluorophore anisotropy. When the 17-base oligonucleotide is bound by protein, the proximity of the bound protein could interfere with the free rotation of the fluorophore about its linker, reducing the local motion and increasing anisotropy. When the 3′-labeled 22-base oligonucleotide is bound, the distance between protein and fluorophore may be greater, increasing fluorophore mobility and reducing ϕ_2.

A third possibility is that the differences between the anisotropic characteristics of the 3′-labeled oligonucleotides reflect effects of DNA sequence on the TAMRA fluorophore. Tetramethylrhodamine fluorescence is sensitive to its environment, and its fluorescence can be quenched by guanosine (*37*). The different sequences at the 3′ end of the 17- and 22-base oligonucleotides could result in different anisotropic characteristics of the probe when in the bound versus unbound state, or when bound by R150A versus wild-type TraI36.

The differences in the anisotropic parameters of the R150A-bound and wild-type-bound 3′-labeled 22-base oligonucleotides are relatively subtle, and the difference in their steady-state anisotropy is difficult to explain convincingly with the available data. It it is feasible, however, that substitution of alanine for a large charged amino acid could affect segmental motion of bound DNA or the interactions of a fluorophore with protein or DNA. Regardless of the precise mechanism, the effect of the R150A substitution on the labeled oligonucleotide serves as another example of the sensitivity of a fluorophore to different environments. This sensitivity, combined with results from a simple oligonucleotide cleavage assay, has allowed us to identify R150 as a determinant of ssDNA binding by F TraI, and to identify its role in specifically interacting with DNA bases 3′ to the *nic* site in *oriT*.

ACKNOWLEDGMENT

We thank the Regional Laser and Biotechnology Laboratories facility and its staff for assistance in collecting time-resolved data. We thank Professor Ludwig Brand for insightful discussions of fluorescence and of this manuscript, and Professors Brand, Robert Schleif, and Ernesto Freire for the use of equipment. We also thank Jennifer Stern for discussions of binding assays and for oligonucleotide purification, and the other members of the Schildbach lab for comments on the manuscript.

SUPPORTING INFORMATION AVAILABLE

Circular dichroism spectra and thermal denaturation of R150A and wild-type TraI36 (Figure 1); binding specificity of R150A to 22-base 3′-TAMRA-labeled oligonucleotide (Figure 2); and time-resolved emission intensity of unbound TAMRA-labeled 22-base oligonucleotide (Figure 3), the 22-base oligonucleotide bound by R150A TraI36 (Figure 4), unbound TAMRA-labeled 17-base oligonucleotide (Figure 5), the 17-base oligonucleotide bound by wild-type TraI36 (Figure 6), and the 17-base oligonucleotide bound by R150A TraI36 (Figure 7). This material is available free of charge via the Internet at http://pubs.acs.org.

REFERENCES

1. Firth, N., Ippen-Ihler, K., and Skurray, R. A. (1996) in *Escherichia coli and Salmonella*, 2nd ed. (Neidhardt, F. C., Ed.) pp 2377−2401, ASM Press, Washington, DC.
2. Frost, L. S., Ippen-Ihler, K., and Skurray, R. A. (1994) *Microbiol. Rev. 58*, 162−210.
3. Traxler, B. A., and Minkley, E. G., Jr. (1988) *J. Mol. Biol. 204*, 205−9.
4. Reygers, U., Wessel, R., Muller, H., and Hoffmann-Berling, H. (1991) *EMBO J. 10*, 2689−94.
5. Matson, S. W., Sampson, J. K., and Byrd, D. R. (2001) *J. Biol. Chem. 276*, 2372−2379.
6. Matson, S. W., and Morton, B. S. (1991) *J. Biol. Chem. 266*, 16232−7.
7. Inamoto, S., Fukuda, H., Abo, T., and Ohtsubo, E. (1994) *J. Biochem. (Tokyo) 116*, 838−44.
8. Howard, M. T., Nelson, W. C., and Matson, S. W. (1995) *J. Biol. Chem. 270*, 28381−6.
9. Nelson, W. C., Howard, M. T., Sherman, J. A., and Matson, S. W. (1995) *J. Biol. Chem. 270*, 28374−80.
10. Matson, S. W., Nelson, W. C., and Morton, B. S. (1993) *J. Bacteriol. 175*, 2599−606.
11. Stern, J. C., and Schildbach, J. F. (2001) *Biochemistry 40*, 11586−95.
12. Sherman, J. A., and Matson, S. W. (1994) *J. Biol. Chem. 269*, 26220−6.
13. Benz, I., and Muller, H. (1990) *Eur. J. Biochem. 189*, 267−76.
14. Lahue, E. E., and Matson, S. W. (1990) *J. Bacteriol. 172*, 1385−91.

15. Dash, P. K., Traxler, B. A., Panicker, M. M., Hackney, D. D., and Minkley, E. G., Jr. (1992) *Mol. Microbiol. 6*, 1163−72.
16. Byrd, D. R., and Matson, S. W. (1997) *Mol. Microbiol. 25*, 1011−22.
17. Yoshioka, Y., Fujita, Y., and Ohtsubo, E. (1990) *J. Mol. Biol. 214*, 39−53.
18. Llosa, M., Bolland, S., and de la Cruz, F. (1994) *J. Mol. Biol. 235*, 448−64.
19. Paterson, E. S., More, M. I., Pillay, G., Cellini, C., Woodgate, R., Walker, G. C., Iyer, V. N., and Winans, S. C. (1999) *J. Bacteriol. 181*, 2572−83.
20. Lum, P. L., and Schildbach, J. F. (1999) *J. Biol. Chem. 274*, 19644−8.
21. Sambrook, J., Fritsch, E. F., and Maniatis, F. (1989) *Molecular Cloning: A Laboratory Manual*, 2nd ed., Cold Spring Harbor Laboratory Press, Cold Spring Harbor, NY.
22. Toptygin, D., and Brand, L. (1995) *Anal. Biochem. 224*, 330−8.
23. Toptygin, D., and Brand, L. (1995) *Spectrabind User's Guide*, The Johns Hopkins University, Baltimore, MD.
24. Toptygin, D., Savtchenko, R. S., Meadow, N. D., and Brand, L. (2001) *J. Phys. Chem. B 105*, 2043−2055.
25. Kojima, H., Spataru, N., Kawata, Y., Yano, S., and Vartires, I. (1998) *J. Phys. Chem. B 102*, 9981−9984.
26. Vamosi, G., Gohlke, C., and Clegg, R. M. (1996) *Biophys. J. 71*, 972−94.
27. Calzaferri, G., and Hugentobler, T. (1985) *Chem. Phys. Lett. 121*, 147−153.
28. Vogel, M., Rettig, W., Sens, R., and Drexhage, K. (1988) *Chem. Phys. Lett. 147*, 452−460.
29. Maroncelli, M. (1993) *J. Mol. Liq. 57*, 1−37.
30. Cheng, Y., and Prusoff, W. H. (1973) *Biochem. Pharmacol. 22*, 3099−108.
31. Classen, S., Ruggles, J. A., and Schultz, S. C. (2001) *J. Mol. Biol. 314*, 1113−25.
32. Horvath, M. P., Schweiker, V. L., Bevilacqua, J. M., Ruggles, J. A., and Schultz, S. C. (1998) *Cell 95*, 963−74.
33. Horvath, M. P., and Schultz, S. C. (2001) *J. Mol. Biol. 310*, 367−77.
34. Ding, J., Hayashi, M. K., Zhang, Y., Manche, L., Krainer, A. R., and Xu, R. M. (1999) *Genes Dev. 13*, 1102−15.
35. Paterson, E. S., and Iyer, V. N. (1997) *J. Bacteriol 179*, 5768−76.
36. Lakowicz, J. R. (1999) *Principles of Fluorescence Spectroscopy*, 2nd ed., Kluwer Academic/Plenum Publishers, New York.
37. Sauer, M., Han, K.-T., Muller, R., Nord, S., Schulz, A., Seeger, S., Wolfrum, J., Arden-Jacob, J., Deltau, G., Marx, N. J., Zander, C., and Drexhage, K. H. (1995) *J. Fluoresc. 5*, 247−61.

BI011969I